Controlled Transport and Focusing of Laser-Accelerated Protons with Miniature Magnetic Devices

M. Schollmeier,[1] S. Becker,[2] M. Geißel,[3] K. A. Flippo,[4] A. Blažević,[5] S. A. Gaillard,[4,6] D. C. Gautier,[4] F. Grüner,[2] K. Harres,[1] M. Kimmel,[3] F. Nürnberg,[1] P. Rambo,[3] U. Schramm,[7] J. Schreiber,[2] J. Schütrumpf,[1] J. Schwarz,[3] N. A. Tahir,[5] B. Atherton,[3] D. Habs,[2] B. M. Hegelich,[2,4] and M. Roth[1]

[1]*Institut für Kernphysik, Technische Universität Darmstadt, Schloßgartenstrasse 9, D-64289 Darmstadt, Germany*
[2]*Department für Physik, Ludwig-Maximilians Universität München, Am Coulombwall 1, D-85748 Garching, Germany*
[3]*Sandia National Laboratories, Albuquerque, New Mexico 87185, USA*
[4]*Los Alamos National Laboratory, Los Alamos, New Mexico 87545, USA*
[5]*GSI—Gesellschaft für Schwerionenforschung mbH, Plasmaphysik, Planckstrasse 1, D-64291 Darmstadt, Germany*
[6]*Physics Department, University of Nevada, Reno, MS220, Reno, Nevada 89557, USA*
[7]*Forschungszentrum Dresden–Rossendorf, Bautzner Landstraße 128, D-01328 Dresden, Germany*

(Received 17 April 2008; published 1 August 2008)

This Letter demonstrates the transporting and focusing of laser-accelerated 14 MeV protons by permanent magnet miniature quadrupole lenses providing field gradients of up to 500 T/m. The approach is highly reproducible and predictable, leading to a focal spot of (286×173) μm full width at half maximum 50 cm behind the source. It decouples the relativistic laser-proton acceleration from the beam transport, paving the way to optimize both separately. The collimation and the subsequent energy selection obtained are perfectly applicable for upcoming high-energy, high-repetition rate laser systems.

DOI: 10.1103/PhysRevLett.101.055004 PACS numbers: 52.38.Kd, 41.85.Lc, 52.59.−f

The realization of intense and energetic laser pulses has resulted in enormous scientific activity over the past decade due to many potential applications including the generation of giga-electron-volt, narrow band electron pulses [1], intense x-ray pulses [2], laser-driven nuclear phenomena [3], inertial fusion energy [4,5], as well as the acceleration of protons from hydrocarbon impurities and heavy ions to mega-electron-volt energies from thin foil targets [6–9]. These ion beams (particularly protons) are generated in a very robust and reproducible way with up to 10^{13} protons by the target normal sheath acceleration mechanism [10]. The ions are accelerated, forming a quasineutral plasma with an exponential energy spectrum that exhibits a sharp cutoff at its maximum energy [11]. Unlike conventionally accelerated ion beams, they contain very high particle numbers in short, picosecond pulses and have unprecedented emittance; i.e., the beams expand in a very laminar fashion [12]. These features make them useful as a diagnostic tool (e.g., proton radiography of transient processes [13]) and they could have applications as compact particle accelerators [14] for the creation of high-energy density (HED) matter [15] or for proton fast ignition [5].

There have been attempts to optimize the source for a more monochromatic beam by using a very thin proton- or carbon-rich layer on the target rear side [16,17]. But, especially for the latter applications, a collimated or focused beam, that maintains the high particle number emitted from a usual foil, is indispensable. Since the beam is divergent with an energy-dependent half-opening angle of up to 40° [18], there have been attempts at ballistic focusing by curving the target foil to a submillimeter half-sphere [15]. However, the focal length is on the order of the sphere's radius, limiting its application. Another possibility for focusing the protons is the ultrafast laser-driven microlens [19] that uses a second laser pulse to create a hot plasma expansion towards the axis of symmetry inside a tiny cylinder. The rapidly varying electric field of the plasma is used to focus traversing protons. The experimental scheme suffers from a complicated geometry with two synchronized high-intensity laser beams that need to be carefully aligned and temporally adjusted. Kar *et al.* [20] recently succeeded in partly collimating the proton beam by combining a microlens device with a flat target foil into a single piece, at the expense of a complex target assembly.

In this Letter an alternative and straightforward approach is presented that uses an ion optical system consisting of novel permanent magnet miniature quadrupoles (PMQ) with strong field gradients of up to 500 T/m, originally developed for laser-accelerated electrons [21]. A set of two PMQs demonstrates transport and focusing of laser-accelerated protons in a very reproducible and predictable manner. This approach uses permanent magnets that do not need to be replaced, hence allowing the application in upcoming high-energy, high-repetition rate lasers. Moreover, it decouples the acceleration process from the beam transport, allowing for independent optimization of the proton beam generation and of the focusing mechanism.

An initial experiment was carried out at the TRIDENT chirped pulse amplification (CPA) laser system at Los Alamos National Laboratory, and obtained a line focus, whereas the demonstration experiments with a point focus were carried out at the *Z*-Petawatt at Sandia National Laboratories (SNL) [22]. The CPA laser at SNL with a wavelength of 1053 nm delivered 40 J laser energy on target, focused by an off-axis parabolic mirror to a beam

spot of 5 μm FWHM. With a pulse duration less than 1 ps, the intensity on the target front side was $I > 5 \times 10^{19}$ W/cm^2. The prepulse contrast ratio was measured as 10^{-7}. A 25 μm thin Cu foil was used as the target, being hit by the p-polarized laser at an angle of 45°. The accelerated protons were detected with a stack of calibrated radiochromic films (RCF) [23]. The calibration for proton energy deposition was done at the tandem linear accelerator at the Max-Planck-Institut für Kernphysik in Heidelberg, Germany. The stacks in the experiment consisted of eight layers of type HD-810 and nine layers of MD-V2-55. Parasitic radiation and target debris require the RCF stacks to be wrapped in 16.3 μm aluminum foil for shielding. The energy-loss response functions of the stacks were calculated with a ray-tracing algorithm using energy-loss values from SRIM-2006 [24], taking into account the different material compositions of the different types of RCF. Because of the Bragg peak of the ion's energy loss at the end of their range, each RCF layer can be attributed to a small energy interval of 1 MeV for MD-V2-55 and 0.5 MeV for HD-810, respectively. Hence, a stack of RCF layers is a two-dimensional imaging spectrometer.

The experimental configuration is shown in Fig. 1. One RCF stack was placed at (40 ± 1) mm behind the target, detecting the divergent proton beam. The axial aperture was 5 mm throughout the PMQ beam transport section. Beam blocks consisting of 12.7 mm aluminum or 6.35 mm stainless steel protected the PMQs from debris and unwanted irradiation. The magnetic fields were calculated using a Maxwell-compliant solver for their specific design [25]. These fields were used to determine the positions of the PMQs and the spectrometer with a tracking algorithm [26]. The goal was to focus 14 MeV protons, since this energy is in the central region of the proton energy spectrum usually produced at TRIDENT and Z-Petawatt. The first PMQ was placed at a distance of 170 mm behind the target and the second one was placed at 230 mm. The focal spot was expected 500 mm behind the target, where another RCF stack was placed.

Protons from hydrocarbon contaminations at the foil's rear side were accelerated up to well above 22 MeV, which

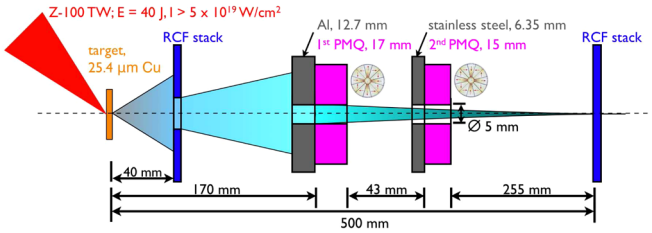

FIG. 1 (color online). Scheme of the experimental setup. A high-intensity laser pulse irradiates a Cu foil. Protons from the rear side propagate into a RCF stack with a 5 mm axial aperture for the detection of the initial beam. The transmitted protons enter two PMQ devices that transport and focus the beam. Another RCF stack in the focal plane records the intensity distribution of the protons.

is the upper detection limit of the RCF stacks used. Although RCF is sensitive to all ionizing radiation, it is most sensitive to protons due to their higher stopping power compared to electrons or x rays. Heavy ions only penetrate the first layer. The total number of protons and their energy spectrum were obtained from the first RCF stack by interpolating over the aperture in the center. High-energy protons were stopped in RCF layers at the end of the stack. Some energy, however, is deposited in the layers before. This fact requires each layer to be deconvolved by the nonlinear detector's response functions. The resulting particle number spectrum dN/dE per unit energy follows the shape obtained in Ref. [11], $dN/dE = N_0/(2Ek_BT)^{1/2} \exp[-(2E/k_BT)^{1/2}]$, with parameters $N_0 = 4.9 \times 10^{12}$ and $k_BT = 1.24$ MeV.

A typical beam profile of (14 ± 1) MeV protons is shown in Fig. 2(a). The white spot in the center is due to a hole allowing for the propagation of the protons through the PMQs. The beam profile shows intensity modulations that originate from microcorrugations of the target rear surface [27]. The beam has a diameter of (29.5 ± 2) mm that corresponds to a (20° ± 1.5°) half-opening angle. A summation of the total signal in Fig. 2(a) leads to 1.3×10^{10} protons with (14 ± 1) MeV. About 7.5×10^8 protons entered the PMQs. This number corresponds to 7.5% of the beam injected into the PMQs. The integration over the spectrum yields a conversion efficiency of 1% of the laser energy into protons with energies above 4 MeV, in agreement with Ref. [11]. The focusing effect of (14 ± 1) MeV protons 50 cm behind the target is shown in Fig. 2(b). By integrating over the peak, a total number of 8.4×10^5 protons is obtained. Hence the transmission through the magnets was $8.4 \times 10^5/7.5 \times 10^8 = 0.1\%$. This was expected, since the first PMQ focused the beam in one plane and defocused the protons in the perpendicular one. The second PMQ's aperture then cut most of the beam.

Although the PMQs were not especially designed for this beam, a small focal spot was obtained. The spot size was by far not limited by the emittance, which is on the order of $10^{-3}\pi$ mm mrad [12]. Simulation results show good agreement with the experiment [Fig. 2(c)]. The RCF was simulated using protons with a Gaussian initial energy distribution of $E = 14$ MeV and standard deviation $\sigma = 1$ MeV. The PMQ's aperture encircles the solid angle of the ion beam by orders of magnitude, justifying the assumption of a uniform initial particle distribution within a much smaller solid angle in order to achieve the best possible statistics for the simulation. The number of macroparticles was 10^6. Interactions (i.e., space charge) were neglected. The horizontal and vertical lineouts of both experiment and simulation (Fig. 3) can be well described by a Lorentzian $f(x) = \sigma/(x^2 + \sigma^2)$ with FWHM $2\sigma = 286$ μm (173 μm) horizontally (vertically), which corresponds to a decrease of the proton beam compared to an unfocused beam of approximately 10^3 times. An estimate based on the simulations for an optimized setup suggests a

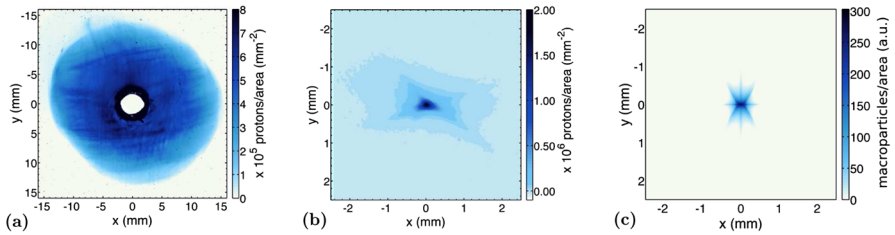

FIG. 2 (color online). (a) Beam profile of (14 ± 1) MeV protons at 40 mm behind the target. The white disk in the center is due to a hole allowing for the propagation of the protons through the PMQs. (b) Beam spot 500 mm behind the target. 8.4×10^5 protons were focused to a small spot by the PMQs. The color map in (b) was optimized to show the weak background signal; therefore, the film appears to have a signal over the whole area. (c) The simulation with a tracking code neglecting emittance shows good agreement with the experiment. The respective RCF was simulated using (14 ± 1) MeV protons.

decrease in the focal spot by an additional factor of 5 in both planes, leading to a demagnification by a factor of $5 \times 5 \times 10^3 = 2.5 \times 10^4$.

Such a small focus is still below the space-charge limit, which can be estimated by the generalized perveance, entrance radius, and focal spot size [28]. Assuming a pulse duration of 0.7 ns from the drift difference of (14 ± 1) MeV protons, the space-charge limit for an optimized focus with 5 mm aperture PMQs corresponds to $\approx 10^9$ protons.

The chromatic properties of PMQs yield an energy-dependent focal spot size. Figure 4(a) shows the ion energy spectrum integrated over an area of 200 μm in diameter. The circles represent the measured data using the PMQ doublet and the solid red line displays the calculated proton spectrum for comparison, using the first RCF stack, under the assumption of an undisturbed propagation of the beam to the same distance. The energy-dependent flux increase due to the focusing is shown in Fig. 4(b). For this specific PMQ configuration, the flux increase for (14 ± 1) MeV protons peaked at about a factor of 75. This allows the system to be used as a spatial filter in order to monochromatize the ion energy spectrum. For an optimization and increased coupling efficiency into the ion optics section, the magnets can be placed closer to the source in combination with an increased aperture of the second PMQ. The latter becomes necessary due to defocusing of the first PMQ in one plane, as well as the space-charge limitation mentioned above that decreases with increasing entrance radius.

Since the ions are emitted in the form of a quasineutral plasma, the question arises of whether or not the copropagating electrons can be safely removed close to the source without distorting the beam, i.e., without increasing the emittance. This was tested experimentally by placing a dipole magnet with 150 mT field strength at a distance of 3 mm behind the target to deflect the electrons, similar to the experiment in Ref. [12], but in our case the magnet was placed much closer to the proton source. A fine mesh (110 μm wire distance, 35 μm wire thickness) that imprints in the beam [29] was placed at the dipole entrance. The protons were recorded with a RCF stack after a drift of 100 mm. The absence of electrons could lead to space-charge forces that diminish the beam quality. However, the image showed a clear imprint of the mesh without any distortion; hence, the beam quality was unchanged. One-dimensional particle-in-cell simulations with the plasma simulation code (PSC) [30] support these findings and show that the magnetic field was sufficient to remove the comoving electrons. Both measurement and simulation demonstrate that even as close as 3 mm from the target a magnetic field can be used to control and transport the ion beam.

These results open up a realm of possibilities for applications; for instance, with an optimized configuration, the transport and focusing of all ions within a certain energy interval could be obtained. It could be used for studies of HED matter by focusing these ions to a small beam spot. The PMQs would allow for a large distance between the proton-production foil and the sample, hence for clean experiments since possible preheating by high-energy photons and electrons [31] would be significantly reduced. As

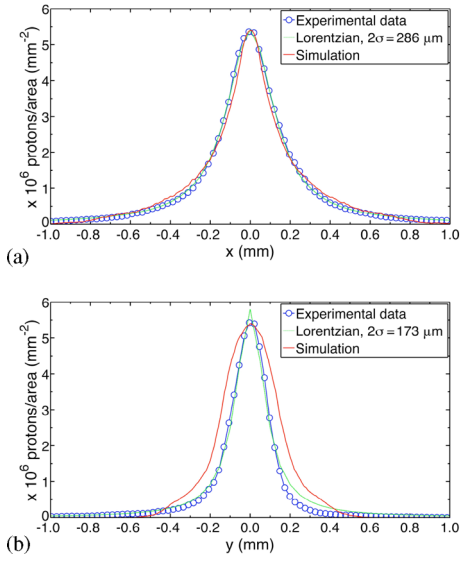

FIG. 3 (color online). Intensity profiles through the beam spot in Fig. 2. The circles show the experimental data, the dark gray (red) lines represent a lineout through the simulated beam profile. Both curves agree well with Lorentzian fits [light gray (green) lines] with a FWHM of $2\sigma = 286$ μm horizontally (a) and even 173 μm vertically (b).

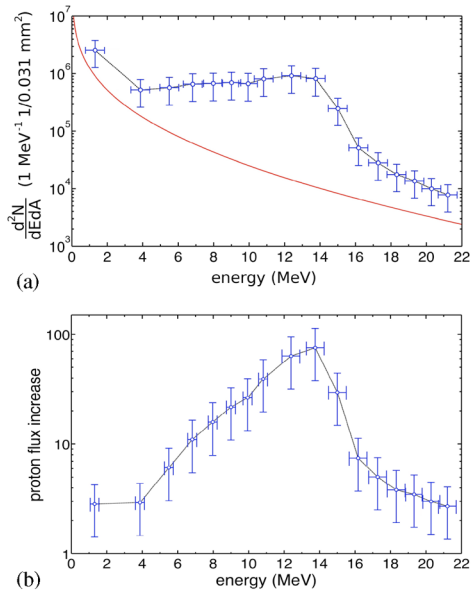

FIG. 4 (color online). (a) 500 mm behind the target the proton beam without the PMQs exhibits an exponentially decreasing spectrum (red solid line). The curve was fit to the RCF data in front of the PMQs adjusted under the assumption of an undisturbed propagation. The spectrum achieved with PMQs (circles) shows a strong signal enhancement which peaks at the designed energy of 14 MeV. (b) The peak of the energy-dependent proton flux increase at 14 MeV shows nearly 75 times more protons per area compared to the case without magnetic lenses.

an example, the HED state of matter that is exposed to 10^{11} protons with 15 MeV, focused to a small spot of 10 μm diameter, was calculated with a semiempirical equation-of-state model [32]. 10 μm thin Al, Ni, and Pb foils were chosen to sample matter from low to high nuclear charge. The energy of the protons is sufficient to penetrate the foil, and the energy deposition is very homogeneous since the Bragg peak is outside the foil. The total specific energy deposition is 505.6 kJ/g for Al, 409.3 kJ/g for Ni, and 277 kJ/g for Pb, respectively. The fast energy deposition by the protons leads to an isochoric heating that transforms the former solid foil to liquid HED matter with temperatures around 20 eV/k_B and around 10 Mbar pressure. This extreme state of matter could be found inside giant planets like Jupiter or Saturn.

In conclusion, the first transport and focusing of laser-accelerated protons with magnetic quadrupole lenses has been shown, which demonstrates the manipulation of laser-accelerated protons by magnetic fields can be done easily, even though the protons are emitted in a quasineutral plasma from the source. The further development and optimization of the magnetic beam transport and focusing system could have significant impact in various areas such as accelerator physics, inertial fusion energy, astrophysics, or even radio oncology (e.g., laser-accelerated hadron therapy for tumor treatment).

We acknowledge the expert support from the TRIDENT and *Z*-Petawatt laser facilities. M. S. thanks H. Ruhl for the PSC. The Darmstadt and Munich groups are supported by VI-VH-144 (VIPBUL). K. A. F., D. C. G., and B. M. H. were funded under LANL Laboratory Directed Research and Development Program, LDRD-DR No. 20040064. Sandia is operated by Lockheed Martin Corp. for the U.S. DOE (Contract No. DE-AC04-94AL85000). S. A. G. is funded under U.S. DOE Grant No. DE-FC52-01NV14050. The Munich group is supported by DFG TR18 and by the Munich Center for Advanced Photonics MAP.

[1] W. P. Leemans *et al.*, Nature Phys. **2**, 696 (2006).
[2] M. M. Murnane *et al.*, Science **251**, 531 (1991).
[3] K. W. D. Ledingham *et al.*, Science **300**, 1107 (2003).
[4] M. Tabak *et al.*, Phys. Plasmas **1**, 1626 (1994).
[5] M. Roth *et al.*, Phys. Rev. Lett. **86**, 436 (2001).
[6] R. A. Snavely *et al.*, Phys. Rev. Lett. **85**, 2945 (2000).
[7] E. L. Clark *et al.*, Phys. Rev. Lett. **84**, 670 (2000).
[8] A. Maksimchuk *et al.*, Phys. Rev. Lett. **84**, 4108 (2000).
[9] M. Hegelich *et al.*, Phys. Rev. Lett. **89**, 085002 (2002).
[10] S. C. Wilks *et al.*, Phys. Plasmas **8**, 542 (2001).
[11] J. Fuchs *et al.*, Nature Phys. **2**, 48 (2006).
[12] T. E. Cowan *et al.*, Phys. Rev. Lett. **92**, 204801 (2004).
[13] L. Romagnani *et al.*, Phys. Rev. Lett. **95**, 195001 (2005).
[14] A. Pukhov, Phys. Rev. Lett. **86**, 3562 (2001).
[15] P. K. Patel *et al.*, Phys. Rev. Lett. **91**, 125004 (2003).
[16] B. M. Hegelich *et al.*, Nature (London) **439**, 441 (2006).
[17] H. Schwoerer *et al.*, Nature (London) **439**, 445 (2006).
[18] M. Zepf *et al.*, Phys. Rev. Lett. **90**, 064801 (2003).
[19] T. Toncian *et al.*, Science **312**, 410 (2006).
[20] S. Kar *et al.*, Phys. Rev. Lett. **100**, 105004 (2008).
[21] T. Eichner *et al.*, Phys. Rev. ST Accel. Beams **10**, 082401 (2007).
[22] J. Schwarz *et al.*, J. Phys. Conf. Ser. **112**, 032020 (2008).
[23] GAFchromic radiochromic film types HD-810 and MD-V2-55 are trademarks of ISP corporation.
[24] J. F. Ziegler, J. P. Biersack, and U. Littmark, *The Stopping and Range of Ions in Solids* (Pergamon, New York, 1985).
[25] CST GmbH, http://www.cst.com.
[26] Pulsar Physics, http://www.pulsar.nl.
[27] M. Roth *et al.*, Phys. Rev. ST Accel. Beams **5**, 061301 (2002).
[28] S. Humphries, Jr., *Charged Particle Beams* (John Wiley and Sons, New York, 1990).
[29] M. Borghesi *et al.* Phys. Rev. Lett. **92**, 055003 (2004).
[30] M. Bonitz, G. Bertsch, V. S. Filinov, and H. Ruhl, *Introduction to Computational Methods in Many Body Physics* (Cambridge University Press, Cambridge, England, 2004).
[31] E. Brambrink *et al.*, Phys. Rev. E **75**, 065401(R) (2007).
[32] A. V. Bushman, I. V. Lomonosov, and V. E. Fortov, *Equations of State for Materials at High Energy Density* (Institute of Problems of Chemical Physics, Moskow, Chernogolovka, 1992), in Russian.